Dynamical correlation of non-stationary signals in time domain—A comparative study

M. Muthuraman [a,b,*], A. Galka [b], G. Deuschl [b], U. Heute [a], J. Raethjen [b]

[a] *Institute for Circuit and System Theory, Faculty of Engineering, University of Kiel, Kaiserstrasse 2, D-24143 Kiel, Germany*
[b] *Department of Neurology, University of Kiel, Schittenhelmstrasse 10, 24105 Kiel, Germany*

1. Introduction

The frequency content of biological signals is typically analysed by digital spectral analysis. The traditional approach is the discrete Fourier transform performed for all the segments of the data under study. The resulting periodograms [1] are then averaged leading to a smooth power spectrum, which allows a smaller variance of the estimate of the frequency content of the investigated signal. However, this approach has important limitations. If the size of the data segments used for the analysis is small, the frequency resolution decreases proportionally. On the other hand, the larger the number of segments, the smoother the power spectrum and less variant is the spectral estimation. Thus there is a trade-off between smoothness of spectral estimation and frequency resolution which is especially problematic when applied to short data lengths. For the same reason the application of methods to short intervals of data is limited and the analysis of temporal evolution of spectral power in different frequency bands lacks temporal resolution. Due to these limitations, alternative methods for reliable spectral estimation for very short intervals of data have been developed. The most commonly used approach is the continuous wavelet transform [2]. In its original form the temporal resolution of the wavelet-transform decreases with the frequency of interest. Thus for low frequencies the time resolution is poor. Recent extensions of the wavelet

* Corresponding author at: Institute for Circuit and System Theory, Faculty of Engineering, University of Kiel, Kaiserstrasse 2, D-24143 Kiel, Germany.
Tel.: +49 431 328 9984; fax: +49 431 880 6128.
E-mail address: mm@tf.uni-kiel.de (M. Muthuraman).

method have, however, made it possible to obtain the same temporal resolution for all frequency bands [3]. Another method for highly time-resolved spectral analysis is the multitaper method [4] which uses more than one window ('taper') for analysing the signal. This method has been introduced into the analysis of biological data more recently and also performs with high temporal resolution irrespective of the frequency bands under study. Thus both methods allow assessing the dynamical changes in spectral and cross-spectral estimates over time.

For biological questions it is often important to detect even very short-time intervals during which the power or coherence in a specific frequency range drops or disappears [5]. It has been postulated that the cortex may only be intermittently involved in the generation of pathological tremors [6] and that the different tremor components at the basic and the "first harmonic" frequencies show distinct dynamics likely indicating separate origins [7,8]. To find out which of the two time-frequency-analysis methods is better to test for such hypotheses, we investigated their performances in two model systems with built-in short drops in power and coherence and in real biological samples of EEG and EMG data recorded from patients with Parkinsonian tremor. The paper is organised as follows: In Section 2 the data acquisition is described. In Section 3 the analysis methods, namely the multitaper and the CWT approaches, are explained. In Section 4 the results of applying the methods to the two model systems are followed by the application to the Parkinsonian data. In Section 5, the methodological advantages and drawbacks of both methods are discussed, and finally, the biological findings on the Parkinsonian data are summarized.

2. Data recordings

In this study we have taken five patients with definite Parkinson's disease as diagnosed by the brain-bank criteria [9]. Patients were seated comfortably in an arm chair with their forearms supported on and their hands hanging freely from the armrests. Surface EMG was recorded from the forearm extensors and flexors on the more affected side with two silver-chloride electrodes positioned close to the motor points of both muscles. EEG was recorded in parallel with a standard 64-channel EEG recording system (Neuroscan, Herndon, VA, USA) using a linked mastoid reference. A standard EEG cap was used with electrode positions according to the extended 10–20 system. EEG and EMG were band-pass filtered (EMG 30–200 Hz; EEG 0.05–200 Hz) and sampled at 1000 Hz. Data were stored in a computer and analysed off-line. Individual recordings were of 1–3 min duration. The number of recordings performed for each patient varied between 3 and 9 depending on the comfort of the subject. The EMG was full-wave rectified. The combination of band-pass filtering and rectification is the common demodulation procedure for tremor EMG [10]. The EEG was made reference-free by a Hjorth transformation [11]. The practical implementation of the Laplace operator detects source activity as it appears at the surface level of the scalp. It is realized in the 10–20 system of electrode placement basically as an analogue superposition of four bipolar derivations, forming a star-like configuration around each electrode. The 64-channel layout was used for recording the EEG. But only 49 electrodes were recorded and used for the Hjorth transformation and finally we derive 35 electrodes excluding the 14 boundary electrodes.

3. Analysis methods

3.1. Multitaper method

In this method the spectrum is estimated by multiplying the data with K different windows (i.e. tapers). The method uses a sliding time window for calculating the power spectrum by discrete Fourier transformation. If $x(t)$ is the signal, then the spectral power is calculated as follows [12]:

$$S_{\mathrm{MT}}(f) = \frac{1}{K}\sum_{k=1}^{K}|\tilde{X}_k(f)|^2 \tag{1}$$

$\tilde{X}_k(f)$ is the Fourier transform of the windowed signal $x(t)$ which can be calculated as

$$\tilde{X}_k(f) = \sum_{t=1}^{N} w_k(t)x(t)\exp(-2\pi i f t), \tag{2}$$

and the terms $w_k(t)(k = 1, 2, \ldots, K)$ are the K orthogonal tapers. In this study, $K = 7$ tapers were used. As orthogonal tapers with good leakage and spectral properties, the discrete prolate spheroidal sequences (DPSS) [13] are applied.

The DPSS can be defined as $v_k(t, W, N)$, where the kth DPSS has a length N and a frequency-bandwidth parameter W. The Fourier transform of the sequence $v_k(t, W, N)$ is given as

$$U(f) = \sum_{t=1}^{N} v_k(t, W, N)\exp(-2\pi i f t). \tag{3}$$

The K sequences $v_k(t, W, N)$ are determined such that the spectral amplitude $U(f)$ is maximally concentrated in the interval $[-W, W]$, i.e.,

$$\int_{-W}^{W}|U(f)|^2\,df \tag{4}$$

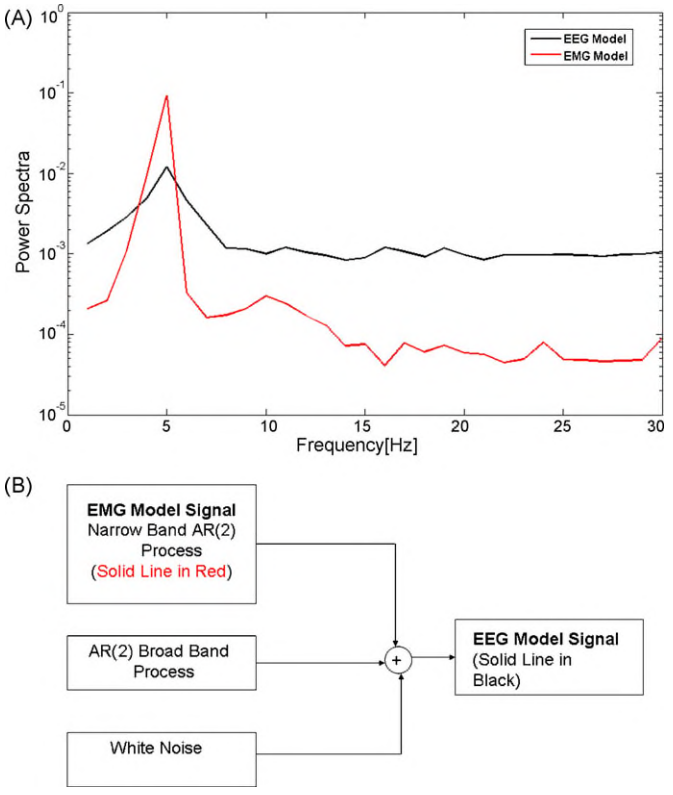

Fig. 1. The power spectrum of the Autoregressive 2nd-order process signals are depicted in (A) solid line in red is the model for the EMG signal, solid line in black is the modeled EEG signal. For clarity the flowchart of the model is depicted in (B). (For interpretation of the references to color in this figure legend, the reader is referred to the web version of the article.)

is maximised. The maximisation problem is solved by using Lagrange multipliers; this leads to an eigenvalue equation, and the eigenvectors of this equation will be the DPSS.

After calculating the power spectra, the coherence between the two signals from the Parkinsonian tremor, in our case the EEG signal $x(t)$ and the EMG signal $y(t)$, is estimated as follows [14]:

$$\hat{C}(f) = \frac{|\hat{S}_{xy}(f)|^2}{\hat{S}_{xx}(f)\hat{S}_{yy}(f)} \tag{5}$$

Here $S_{xy}(f)$ is the cross spectrum and is defined as

$$S_{xy}(f) = \tilde{X}_k(f) \cdot \tilde{Y}_k(f) \tag{6}$$

and estimated as given in Eq. (1). $S_{xx}(f)$, $S_{yy}(f)$ are the individual power spectra estimated as given in the above Eqs. (1) and (2), the overcap indicating the estimation [15]. The coherence is a linear measure between 0 and 1. When the estimated value for the coherence at a frequency is 0, this indicates the lack of correlation between the two signals at this frequency. The value 1 indicates complete correlation between the two signals at this frequency.

In this study, we used windows of length 1000 ms in order to find the intermittent drop in the power for the model system and for the Parkinsonian tremor within a frequency band of 2–30 Hz. The signals were sampled at 1000 Hz, and the time step was 50 ms with overlapping windows. So, in this sense the time resolution is 50 ms, and the frequency resolution is 1 Hz.

3.2. Wavelet-transform method

In this method the Morlet wavelet is used. This is a complex sinusoid windowed with a Gaussian envelope [3]:

$$h(t) = \exp(jct)\exp\left(\frac{-\alpha t^2}{2}\right) \tag{7}$$

The continuous wavelet transform for a continuous signal $x(t)$ can be written as [2]:

$$\mathrm{CWT}_x(\tau, a) = \frac{1}{\sqrt{|a|}} \int x(t) h^* \left(\frac{t-\tau}{a}\right) dt \tag{8}$$

where t and τ are time variables, $h^*(t)$ is the wavelet function, and a is the scaling factor; the constant $1/\sqrt{|a|}$ is used for energy normalisation. The CWT can also be expressed as an integral in the frequency domain [3]:

$$\mathrm{CWT}_x(\tau, a) = \sqrt{|a|} \int_{-\infty}^{\infty} X(u) H^*(ua) \exp(j2\pi u\tau)\, du \tag{9}$$

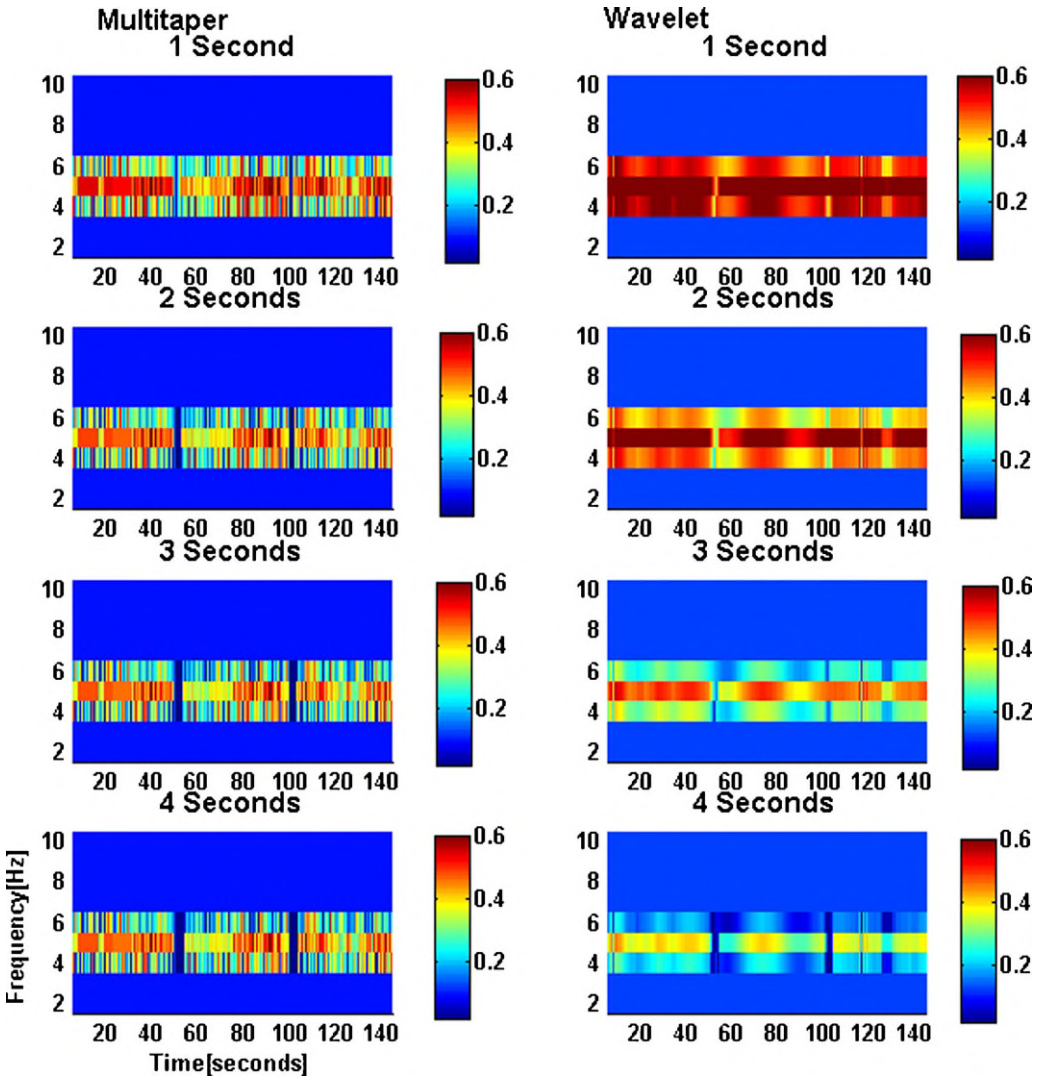

Fig. 2. Estimation of coherence of the coupled autoregressive 2nd-order process model system with incorporated gaps of 1–4 s for the multitaper (left column) and the extended continuous wavelet-transform method (right column) for a single realization.

$X(u)$ and $H(u)$ are the continuous Fourier transforms of the signal $x(t)$ and the wavelet function $h^*(t)$, respectively. The continuous Fourier transform reveals how the energy in the signal $x(t)$ is distributed in frequency. As the scaling factor a is increased, the wavelet function h^* is spread in time, which takes care of long-time oscillations (i.e. low frequency). When the scale is decreased, the function h^* becomes shorter to take care of short-time oscillations (i.e. high frequency). The power is estimated by the square modulus of the CWT, and its representation in time-scale domain is termed scalogram.

The relationship between the scale a and the frequency f can be given as $a = c/f$, where c represents the centre frequency in the wavelet.

To reduce the estimation time, the convolution is done in the frequency domain, as described by Eq. (9). The main feature of the Morlet wavelet is that the relative bandwidth can be easily adjusted using the two parameters c and α. In our case, It is chosen to be $c = 2\pi$ and $\alpha = 0.151$. The relation between these two parameters to the frequency is given by

$$\frac{\sqrt{\alpha}}{c} = \frac{\Delta f}{2\sqrt{2}f} \tag{10}$$

where Δf is the desired frequency resolution at a given frequency f. In this case the choice of c and α individually are unimportant. The important factor is the ratio $\sqrt{\alpha}/c$, which determines the relative bandwidth:

$$\mathrm{BW}_{\mathrm{rel}} = \frac{\Delta f}{f} = \frac{2\sqrt{2\alpha}}{c} \tag{11}$$

This allows the method to have complete flexibility in setting the CWT to have a particular frequency resolution at any particular frequency.

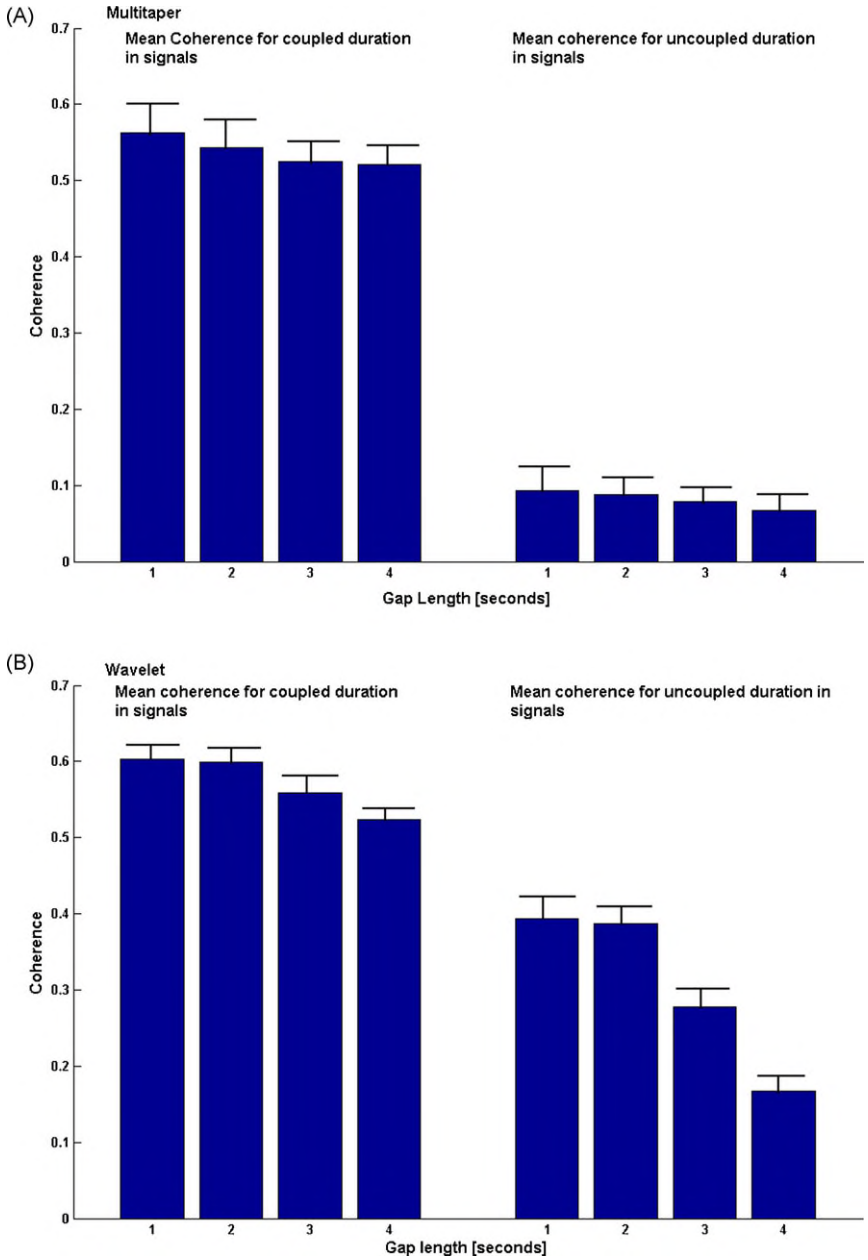

Fig. 3. The mean coherence for all the 10 realizations of the coupled signals from 1 to 4 s for the multitaper method (A) and the wavelet method (B) is calculated as area under the curve for the "coupled time intervals" at 0–50, from 51–100, 52–100, 53–100, 54–100 and 101–150, 102–150, 103–150, 104–150 s and by comparing them with the "uncoupled time intervals" from 50–51, 50–52, 50–53, 50–54 and 100–101, 100–102, 100–103, 100–104 s in the coherence over time and plotted as bar graphs.

In the CWT, we also used windows of length 1000 ms and the time step was 50 ms with overlapping windows. So, in this sense the time resolution is 50 ms, and the frequency resolution is 1 Hz in order to allow a fair comparison of the performance with that of the multitaper method.

4. Results

4.1. Application to model signals for detecting gaps

Both methods were applied to two model systems. One of them was designed using a linear stochastic autoregressive 2nd-order process. The second model was designed using non-linear stochastic van der Pol oscillators. The autoregressive 2nd-order process is defined as

$$y_0(t) = a_1 y_0(t-1) + a_2 y_0(t-2) + \eta_0(t) \tag{12}$$

where a_1 and a_2 are the autoregressive 2nd-order coefficients [16] which are determined as

$$a_1 = 2\cos\left(\frac{2\pi}{T_1}\right)\exp\left(\frac{-1}{T_2}\right) \tag{13}$$

$$a_2 = -\exp\left(\frac{-2}{T_2}\right) \tag{14}$$

In this process, T_1 is the mean oscillation period and T_2 is the relaxation time. $\eta_0(t)$ is a Gaussian white-noise process with zero mean and unit variance. The sampling frequency was chosen to be 1000 Hz again. In Parkinsonian-tremor data, the coherence between concurrently measured EEG and EMG is limited to very narrow bands around 5 Hz and 10 Hz. The varying coherence over time indicates that these frequencies are only intermittently present. For the model signal, we used only one band (5 Hz). A narrow band process was used to model the EMG signal (solid line in red in Fig. 1A). One broad-band (BB) processes were taken and then superimposed on the narrow band process for the whole period of 150 s. This combined process was used as a model for the more broad-band EEG data containing tremor-related activity. Independent white noise was added to the combined process (solid line in black) which is the modelled EEG signal to tune the coherence between 0.25 and 0.6 as it is seen in the biological data. For clarity, the flowchart of the model is given in Fig. 1B. In order to model the intermittent drops in the coherence between EEG and EMG, two gaps of variable length between 0.5 and 4 s where left at 50 and 100 s without superimposition. But the noise process was continued in these gaps. Now, the magnitude of the coherence over time between the two processes should be reduced at these instances for the duration of the gaps.

In order to validate the methods for the application to non-linear systems, an example of coupled stochastic van der Pol oscillators was used [17]. The equations for their descriptions are given as

$$\ddot{x}_1 = \mu(1-x_1^2)\dot{x}_1 - \omega_1^2 x_1 + \sigma\eta_1 + \varepsilon_{12}(x_2 - x_1) \tag{15}$$

$$\ddot{x}_2 = \mu(1-x_2^2)\dot{x}_2 - \omega_2^2 x_2 + \sigma\eta_2 + \varepsilon_{21}(x_1 - x_2) \tag{16}$$

where $\omega_1 = 1.45$, $\omega_2 = 1.48$, and η_i is Gaussian distributed white noise. The interaction between these two oscillators is still linear; the system is non-linear due to the terms which are weighted by the parameter μ. This value is fixed to 5, which leads to a highly non-linear behaviour of the van der Pol oscillators. The coupling factors are fixed to $\varepsilon_{12} = \varepsilon_{21} = 0.25$. The model was investigated with $N = 150{,}000$ data points. The intermittent drops in the coherence were modelled in the same way as in the autoregressive process with two gaps of variable length.

The methods were tested on both model systems for 10 realisations of each gap length (0.5–4 s). The multitaper method was able to exactly identify gaps in the signals as small as 1 second as shown in Fig. 2 for one realisation of the autoregressive 2nd-order process. The minimum detected gaps for all the 10 realisations in

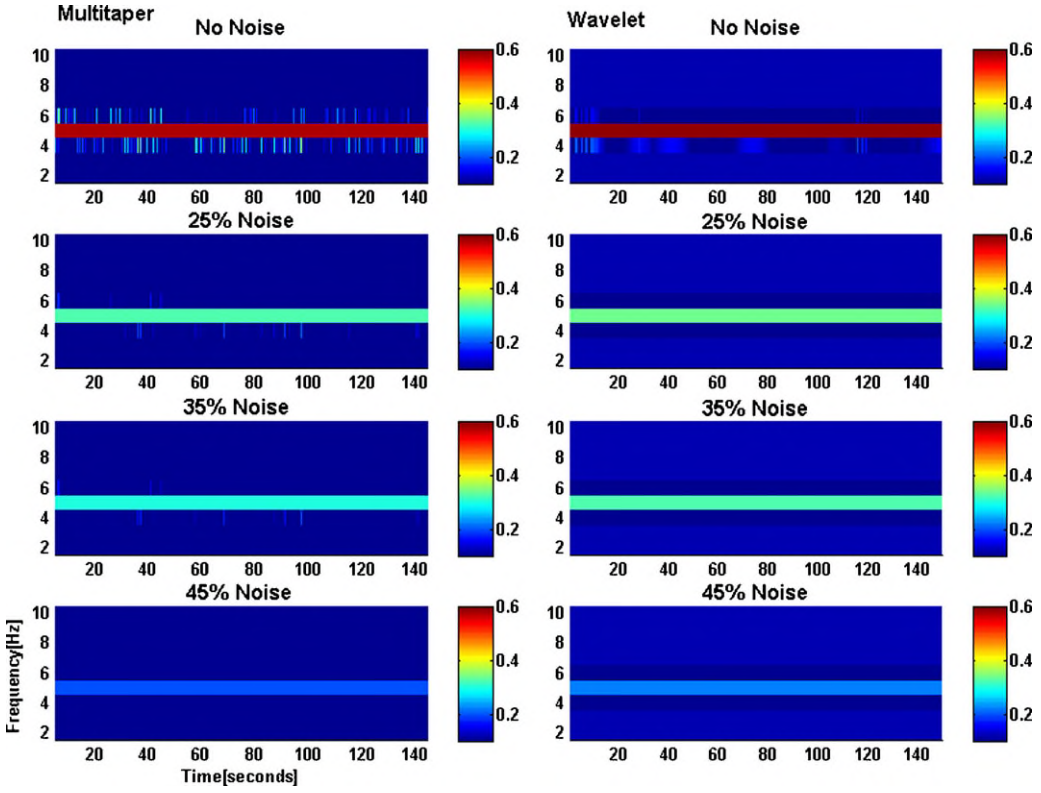

Fig. 4. Estimation of coherence of the coupled van der Pol oscillator model system without additional observational noise followed by addition of noise from 25 to 45% for the multitaper (left column) and the extended continuous wavelet-transform method (right column) for a single realization.

Table 1
The mean and standard deviation of the minimum detected gap for both the model signals.

Minimum detected gap width (s)	MTM	CWT
AR2	0.97 ± 0.10	3.51 ± 0.21
van der Pol	1.12 ± 0.11	3.61 ± 0.19

both model systems are summarised in Table 1 with mean and standard deviation. The 0.5 s gap was not identified, only a small drop in the coherence was seen at these instances in time. In case of the CWT method, gaps below 4 s were not clearly identified as shown in Fig. 2. A finite coherence value remained in all the 10 realisations. The difference in coherence for all the 10 realisations of the autoregressive 2nd-order process for the coupled and uncoupled durations in the signals was estimated by taking the mean coherence in the frequency interval 4–6 Hz for the "coupled time intervals" at 0–50, from 51–100, 52–100, 53–100, 54–100 and 101–150, 102–150, 103–150, 104–150 s and by comparing them with the "uncoupled time intervals" from 50–51, 50–52, 50–53, 50–54 and 100–101, 100–102, 100–103, 100–104 s. The mean coherence with the standard deviation for the gaps from 1–4 s is indicated as bars in Fig. 3. In Fig. 3A the MTM showed a large difference in coherence between the coupled time and the uncoupled time identifying the induced gap in the signals, whereas the extended CWT as displayed in Fig. 3B showed much less difference below 4 s indicating that there is only a slight decrease in the estimated coherence, not reduced to the same degree as in the case of the MTM. The difference between the methods with respect to the factors gap length and coupled or not coupled duration in the signals was tested by the *n*-way analysis of variance (ANOVA) method which showed that all the factors and their interactions were significant ($p < 0.01$). The mean coherence was calculated taking into account all the 10 realisations.

4.2. Application to model signals for random fluctuations

In the two model systems, both processes were added with external observational white noise with a level of 25–75% compared to the signal level, to get the noise threshold of the methods and also to prove that the decrease in coherence is monotonic and not due to random fluctuations in stochastic signals for the whole period. The noise threshold was identified as 45% by visual inspection. For each 10% increase starting from 25% of noise the time-frequency plots for one realisation of the van der Pol oscillators are shown in Fig. 4. The decrease in coherence was monotonic with the increase in noise power over the entire range of 150 s for both model systems. The methods were tested on the autoregressive 2nd-order process and the van der Pol oscillators for 10 realisations with almost identical results for both model system and all realisations.

4.3. Application to Parkinsonian tremor

The methods were now applied to recordings from 5 Parkinson tremor patients all of which showed clear peaks in the corticomuscular coherence at the tremor frequency and the "first harmonic" frequency. The coherence was centered in the central electrodes contralateral to the trembling muscle (EMG) under study. The power spectrum of the left forearm extensor muscle (M4) and the coherence between the EEG electrode C2 and this muscle of a Parkinsonian patient are shown in Fig. 5. The average basic frequency was 4.8 ± 0.8 Hz and the average "first harmonic" frequency was 9 ± 1.58 Hz across all patients and recordings. In all the five patients the contralateral electrode with the highest coherence was taken for the analysis of power and coherence over time.

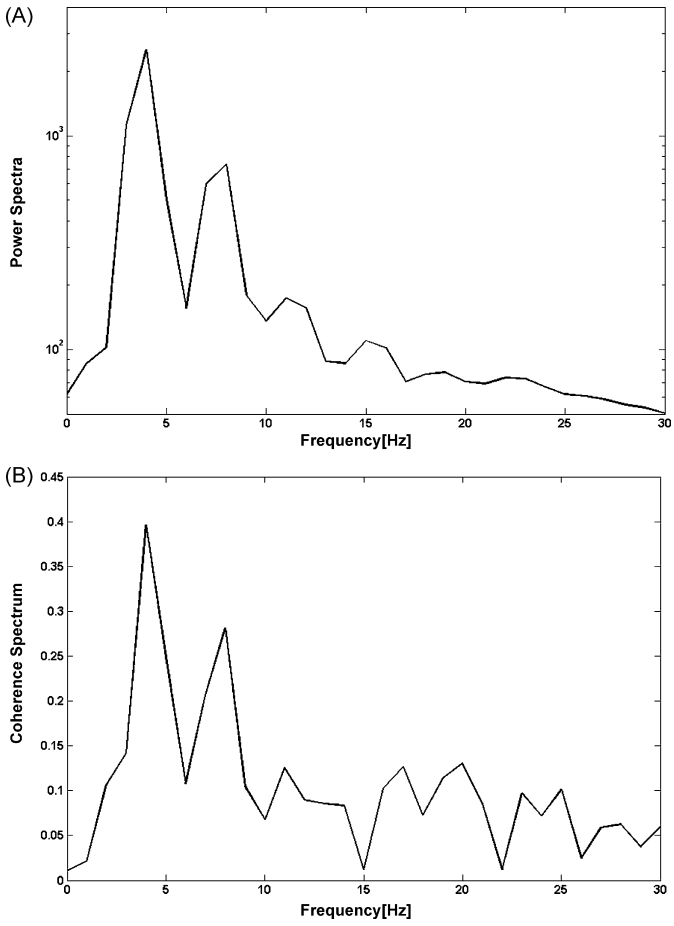

Fig. 5. An example for the typical EMG (forearm extensor) envelope power spectrum in Parkinsonian tremor (A) and the corresponding corticomuscular (EEG–EMG) coherence spectrum (B) for a single recording. The basic tremor frequency 4 Hz and the first harmonic frequency 8 Hz shown by the peaks in the EMG envelope spectrum are both coherent with an EEG (C2) electrode on the contralateral side.

As already seen in the model-signal analysis, the MTM was able to detect relatively short-lived drops in power or coherence in one of the two frequency bands, whereas the CWT tended to smear the estimates. In Fig. 6 (bottom) the power spectrum was estimated from 0 to 25 s using the Welch periodogram method [1]. The basic tremor frequency at 4 Hz and the "first harmonic" frequency at 9 Hz are present at this time interval which is also clearly depicted by both methods in the power-spectrum estimations over time. However, the power spectrum from 95 to 115 s shows only power at the "first harmonic" frequency of 9 Hz. This change is clearly identified by the multitaper method as a gap in power at the basic frequency of 5 Hz. In the extended continuous wavelet transform, the estimation of the power spectrum is smeared over time and indicates high power all the time in both frequencies.

The main finding illustrated in Fig. 6 was that the power and corticomuscular coherence followed distinct time courses at the basic and the higher "harmonic" frequencies with the cortical correlate of one of them often being present without the other. The significant difference between both these frequencies for all the five patients was tested using a surrogate analysis. In order to obtain a 1% significance level, 100 surrogates were estimated with the coherence values taken for every 1 s for the whole period of 150 s. The cross correlation between the two time series was calculated by shuffling the coherence values of both of them randomly for 99 times and then comparing it with the cross correlation of the 100th surrogate, which was calculated with the actual coherence values. The results are shown in Fig. 7 in which the vertical

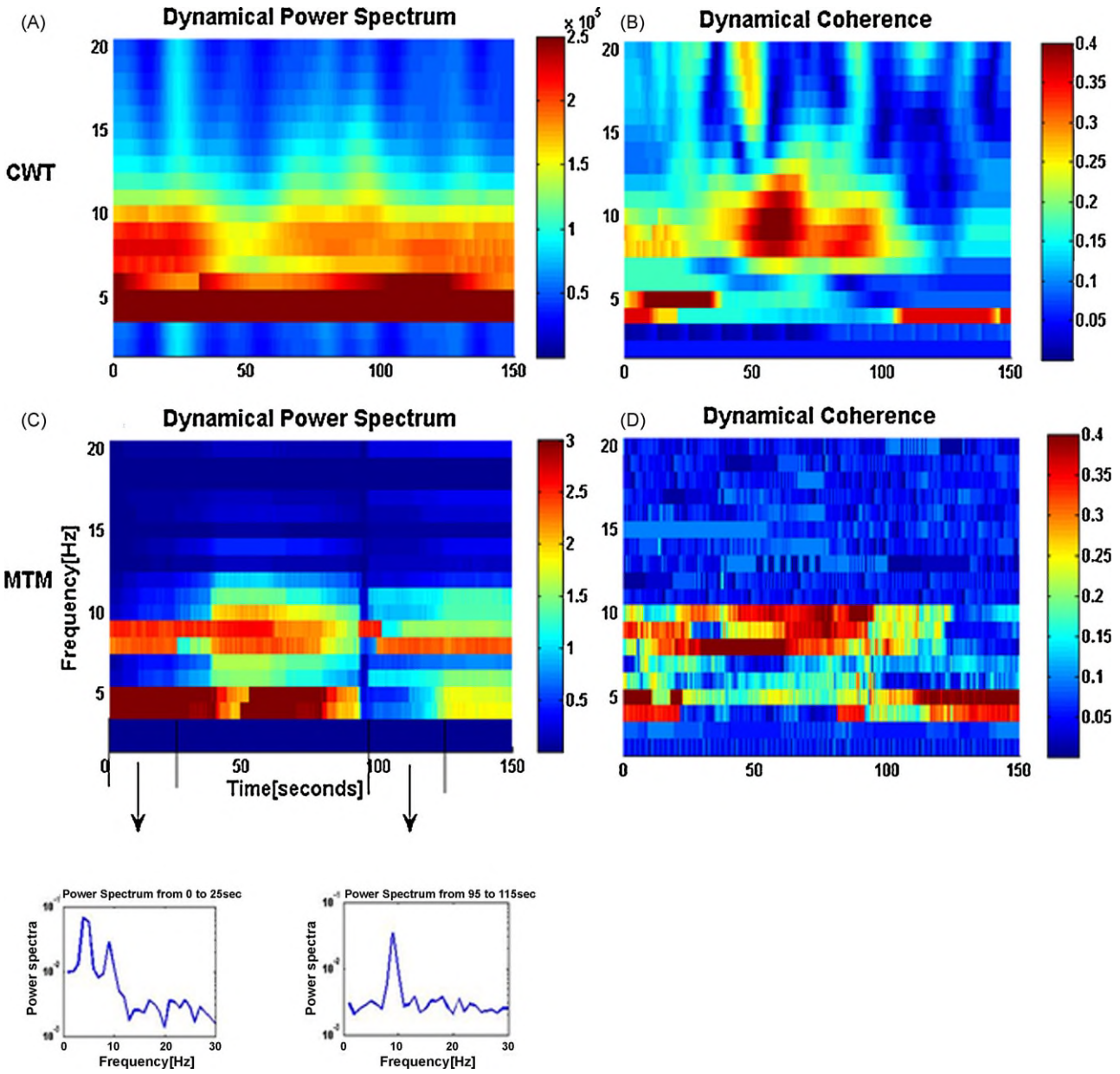

Fig. 6. The dynamical power spectrum of the extensor right muscle-M2 and corticomuscular coherence spectrum between EEG electrode C1 and extensor right muscle-M2 of a Parkinsonian-tremor patient analyzed with extended continuous wavelet-transform method (A and B) and multitaper method (C and D). The power spectra for the time intervals from 0 to 25 s and from 95 to 115 s were estimated by the Welch periodogram method.

dashed lines indicate the cross correlation of the 100th surrogate for the five patients which was negatively correlated compared to the other 99 surrogates which was close to 0. By these results we can confirm that the two frequencies follow significantly distinct time courses and also they are negatively correlated in all the patients.

5. Discussion

The traditional continuous wavelet transform has a varied time-frequency resolution at any position in the time-frequency plane and achieves better time resolution but larger frequency distortion in the upper frequency range [18,19]. In this paper we have used the extended version of the continuous wavelet transform, applying the Morlet wavelet. It has been claimed that this can be used to freely choose an appropriate time-frequency resolution [3] as is the case of the multitaper method. Applying these methods to the model signals revealed that the MTM was able to clearly detect the short-lived gaps of 1–4 s in the power and coherence between two coupled signals. In the case of the extended CWT, gaps below 4 s were not clearly identified in all the 10 realisations. The MTM showed a large difference in coherence between the coupled and uncoupled time segments compared to the extended CWT. This indicates that the MTM is more suitable to analyze the dynamics of the spectral power and coherence with high temporal resolution. Both analyses were tested for their noise thresholds on two model signals, and the thresholds were between 40 and 50% for both methods. It was also proved that the reduction of coherence was monotonic over the whole period.

The main drawback in the wavelet method is that only one Morlet wavelet is used as the template for the whole period of signals. In case of the multitaper method, the (e.g. 7) tapers are different in

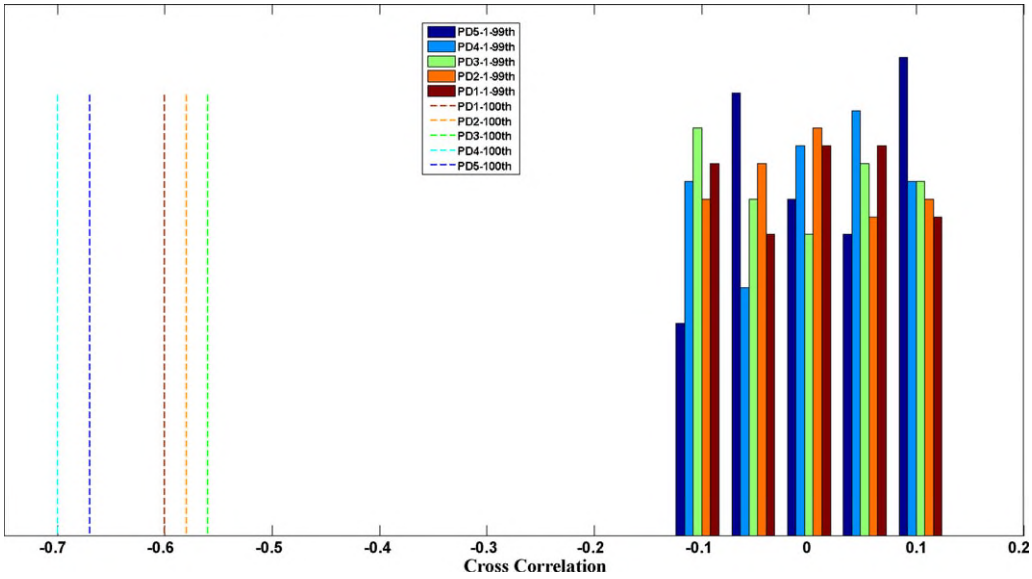

Fig. 7. The distinct nature of the basic and the first harmonic frequency is statistically tested by calculating 99 surrogates with random shuffling of the coherence values followed by the 100th surrogate with the original coherence values. The dashed lines indicate the cross correlation of the 100th surrogate values for the five Parkinsonian subjects which is 1% significant compared to the other values.

shape and all of them are used as windows and multiplied with the signal. The overall information of all the tapers is taken into account for the estimation which gives additional information about the signal. The length of the windows is the same for all the seven tapers and they do not have different pass bands [4]. The window length is identified for all seven tapers. Also, their corresponding frequency responses do not differ strongly in their pass band shapes. Differences do exist, however, in terms of the DC (i.e. zero frequency) amplifications and of the leakage suppression especially at alternating, slightly shifted frequencies. The inherent averaging of the method leads to the advantageous behaviour observed above. The combination of all these windows in the multitaper method gives less leakage about the edges of the signals after windowing and gives a clear indication of the time behaviour, which is very useful in finding the sharp changes in the signals [4]. However, the computation time of the multitaper method on an Intel(R) Pentium(R) M processor 1.70 GHz PC is 10 min compared to one minute for the extended continuous wavelet transform for 150 s of data using Matlab, i.e., a factor of 10 has to be accepted as a price for the better performance.

In the tremor signals, there are multiple components [20] within the low frequency range from 4 to 10 Hz. Resolving these components within such a small frequency range is difficult in case of the wavelet transform, because when there are two frequency components within an analysis time-domain window, the estimation is noisy at these frequencies and tends to overestimate the different components present in the signals. The two frequency components were more reliably separated over the whole time course using the MTM.

Now, based on new insights into the reliability of the analysis, two important aspects of the coupling between EEG and EMG have become clear: They are only coupled at certain intervals in time and the two frequencies involved (basic tremor and "first harmonic" frequencies) have a distinct time course in the coherence over time.

In summary we conclude from the methodological point of view that the MTM is more suitable for analysing the exact dynamics of low frequency multimodal signals than the extended version of CWT. In the biological point of view our results on Parkinsonian tremor support the notion that the basic frequency and "first harmonic" are in fact distinct processes both contributing to the peripheral tremor.

Acknowledgements

Support from the German Research Council (Deutsche Forschungsgemeinschaft, DFG, SFB 855, Project D2) is gratefully acknowledged.

References

[1] P.D. Welch, The use of fast Fourier transform for the estimation of power spectra: a method based on time averaging over short, modified periodograms, IEEE Trans. Audio Electroacoustics 15 (1967) 70–73.
[2] O. Rioul, M. Vetterli, Wavelets and signal processing, IEEE Trans. Signal Process. (1991) 14–38.
[3] A. Metin, Time Frequency and Wavelets in Biomedical Signal Processing, IEEE Press, 1997, pp. 101–115.
[4] D.B. Percival, A.T. Walden, Spectral Analysis for Physical Applications: Multitaper and Conventional Univariate Techniques, Cambridge Univ. Press, Cambridge, UK, 1993, pp. 331–374.
[5] G. Deuschl, P. Bain, M. Brin, Consensus statement of the Movement Disorder Society on tremor, Mov. Disord. 13 (Suppl. 3) (1998) 2–23.
[6] J. Raethjen, R.B. Govindan, F. Kopper, M. Muthuraman, G. Deuschl, Cortical involvement in the generation of essential tremor, J. Neurophysiol. 97 (5) (2007) 3219–3228.
[7] J. Volkmann, M. Joliot, A. Mogilner, A.A. Ioannides, F. Lado, E. Fazzini, U. Ribary, R. Llinas, Central motor loop oscillations in Parkinsonian resting tremor revealed by magnetoencephalography, Neurology 46 (1996) 1359–1370.
[8] L. Timmermann, J. Gross, M. Dirks, J. Volkmann, H.J. Freund, A. Schnitzler, The cerebral oscillatory network of Parkinsonian resting tremor, Brain 126 (2003) 199–212.
[9] A.J. Hughes, S.E. Daniel, L. Kilford, A.J. Lees, Accuracy of clinical diagnosis of idiopathic Parkinson's disease: a clinical-pathological study of 100 cases, J. Neurol. Neurosurg. Psychiatry 55 (3) (1992) 181–184.
[10] H.L. Journee, Demodulation of amplitude modulated noise: a mathematical evaluation of a demodulator for pathological tremor EMG's, IEEE Trans. Biomed. Eng. 30 (5) (1983) 304–308.
[11] B. Hjorth, An on-line transformation of EEG scalp potentials into orthogonal source derivations, Electroencephalogr. Clin. Neurophysiol. 39 (1975) 526–530.
[12] P.P. Mitra, B. Pesaran, Analysis of dynamic brain imaging data, Biophys. J. 76 (1999) 691–708.
[13] D. Slepian, H.O. Pollak, Prolate spheroidal wavefunctions Fourier analysis and uncertainty. I. Bell, Syst. Technol. J. 40 (1961) 43–63.
[14] M.R. Jarvis, P.P. Mitra, Sampling properties of the spectrum and coherency of sequences of action potentials, Neural Comput. 13 (2001) 717–749.
[15] D.M. Halliday, J.R. Rosenberg, A.M. Amjad, P. Breeze, B.A. Conway, S.F. Farmer, A frame work for the analysis of mixed time series point process data—theory and application to study of physiological tremor, single motor unit discharges and electromyogram, Prog. Biophys. Mol. Biol. 64 (1995) 237–238.
[16] M. Lindemann, J. Raethjen, J. Timmer, G. Deuschl, G. Pfister, Delay estimation for cortico-peripheral relations, J. Neurosci. Methods 111 (2) (2001) 127–139.
[17] B. van der, Pol. On oscillation-hysteresis in a simple triode generator, Philos. Mag. 43 (1922) 700–719.

[18] O. Rioul, P. Flandrin, Time-scale energy distributions: a general class extending wavelet transforms, IEEE Trans. Signal Process. 40 (1992) 1746–1757.
[19] Y.W. Shou, Z.A. Tipu, F.S. John, L. Xuguang, Time frequency analysis of transient neuromuscular events: dynamic changes in activity of the subthalamic nucleus and forearm muscles related to the intermittent resting tremor, J. Neurosci. Methods 145 (2005) 151–158.
[20] N. Sapir, R. Karasik, S. Havlin, E. Simon, J.M. Hausdorff, Detecting scaling in the period dynamics of multimodal signals: application to Parkinsonian tremor, Phys. Rev. E 67 (1) (2003) 1–8.